

## Supporting information

### **Two-Dimensional MBene: a comparable catalyst to MXene for effective CO<sub>2</sub>RR towards C<sub>1</sub> products**

Xiaoqing Lu<sup>a\*</sup>, Yuying Hu<sup>a</sup>, Shoufu Cao<sup>a</sup>, Jiao Li<sup>a</sup>, Chunyu Yang<sup>a</sup>, Zengxuan Chen<sup>a</sup>, Shuxian Wei<sup>b\*</sup>, Siyuan Liu<sup>a</sup>, Zhaojie Wang<sup>a\*</sup>

<sup>a</sup> *School of Materials Science and Engineering, China University of Petroleum, Qingdao, Shandong 266580, P. R. China*

<sup>b</sup> *College of Science, China University of Petroleum, Qingdao, Shandong 266580, P. R. China*

\* Corresponding author: Shuxian Wei, Zhaojie Wang, Xiaoqing Lu

E-mail address: wshx@upc.edu.cn, wangzhaojie@upc.edu.cn, luxq@upc.edu.cn

## Computational Methods

### Computational hydrogen electrode model

The free energy diagrams of CO<sub>2</sub>RR were calculated by referring to the computational hydrogen electrode (CHE) model proposed and developed by Norskov et al. The  $\text{H}^+(\text{aq}) + \text{e}^- \rightleftharpoons 1/2 \text{H}_2(\text{g})$  was equilibrated at 0 V versus the reversible hydrogen electrode (RHE).

The Gibbs reaction energy ( $\Delta G$ ) was defined as follows,

$$\Delta G = \Delta E + \Delta E_{\text{ZPE}} + \int C_p dT - T\Delta S + \Delta G_U$$

where  $\Delta E$  was the DFT calculated electronic energy,  $\Delta E_{\text{ZPE}}$ ,  $\int C_p dT$ , and  $\Delta S$  were the zero-point energy, enthalpic temperature correction, and the entropy difference between the products and the reactants, respectively, which were all calculated according to the vibration analysis at room temperature ( $T = 298.15 \text{ K}$ ). For the vibration analysis, frequencies were calculated by treating all 3N degrees of the adsorbates as vibrational in the harmonic oscillator approximation, in which the vibrations of the substrate surface were negligible.  $\Delta G_U$  was the contribution of the applied electrode potential (U) to  $\Delta G$ .

In this model, electrode potential correction to the free energy of each state is included by considering the electrochemical proton-electron transfer being a function of the applied electrical potential. The free energy of a proton-electron pair at 0 V versus RHE is defined to be equal to 1/2 of the H<sub>2</sub> free energy at 101,325 Pa. The free energy of each intermediate, calculated at 298.15 K, is then a function of the electrode potential (U) according to

$$G(U) = G(0V) + neU$$

where  $e$  is the elementary charge of an electron,  $n$  is the number of proton-electron pairs transferred to the investigated intermediate or final states. The application of this equation to the elementary reaction pathway results in the electrode potential corrected free energy pathway, therefore provides a venue to evaluate at which potential a certain CO<sub>2</sub> electroreduction pathway opens, as well as defining the potential dependent reaction step.

## Quantifying Product Selectivity

The selectivity of the competing CO<sub>2</sub>RR and HER is quantified by applying the model reported in reference [1]. For CO<sub>2</sub>RR, four possible C<sub>1</sub> products, CO, HCOOH, CH<sub>3</sub>OH, and CH<sub>4</sub>, are taken into consideration. The ratio of the CO<sub>2</sub>RR and HER current densities,  $j_{\text{CO}_2\text{RR}}/j_{\text{HER}}$ , at 0 V is given by the equation,

$$\frac{j_{\text{CO}_2\text{RR}}(U = 0 \text{ V})}{j_{\text{HER}}} = \text{Exp}\left(\frac{G_{\text{max-HER}}^{\#} - G_{\text{max-CO}_2\text{RR}}^{\#}}{k_{\text{B}}T}\right)$$

In which,  $k_{\text{B}}$  denotes Boltzmann's constant, and T the absolute temperature in Kelvin ( $T = 298.15$  K).

The CO<sub>2</sub>RR selectivity relevant to HER is determined by the following equation:

$$\text{CO}_2\text{RR selectivity} = \frac{\text{Exp}\left(\frac{G_{\text{max-HER}}^{\#} - G_{\text{max-CO}_2\text{RR}}^{\#}}{k_{\text{B}}T}\right)}{\text{Exp}\left(\frac{G_{\text{max-HER}}^{\#} - G_{\text{max-CO}_2\text{RR}}^{\#}}{k_{\text{B}}T}\right) + 1}$$

The free-energy distance of the transition-state free energies,  $G_{\text{max-HER}}^{\#} - G_{\text{max-CO}_2\text{RR}}^{\#}$ , is approximated by assuming a linear decrease of the free-energy spacing of the H intermediate and the CO<sub>2</sub>RR intermediate along the reaction coordinate. Assuming that the activated complexes of the CO<sub>2</sub>RR and HER are located in the middle of the electrochemical double layer ( $\alpha_{\text{CO}_2\text{RR}} = \alpha_{\text{HER}} = 1/2$ ), the following relation holds true:

$$G_{\text{max-HER}}^{\#} - G_{\text{max-CO}_2\text{RR}}^{\#} = 1/2(\Delta G_{\text{max-HER}} - \Delta G_{\text{max-CO}_2\text{RR}})$$

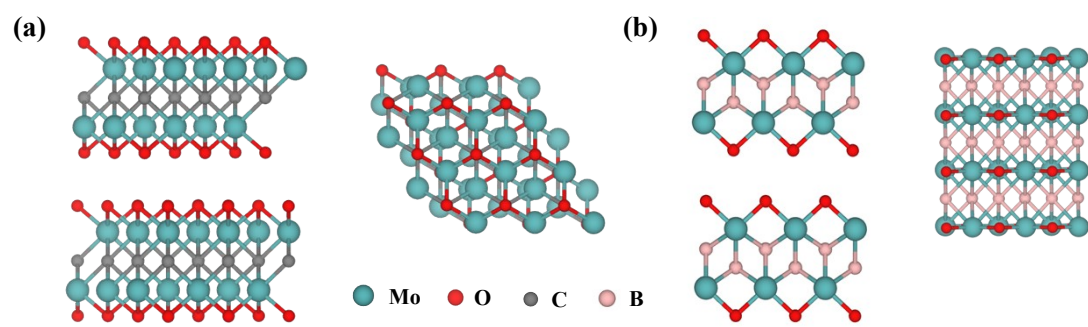


**Figure S1.** Optimized structural model of (a)  $\text{Mo}_2\text{CO}_2$  and (b)  $\text{MoBO}_2$ .

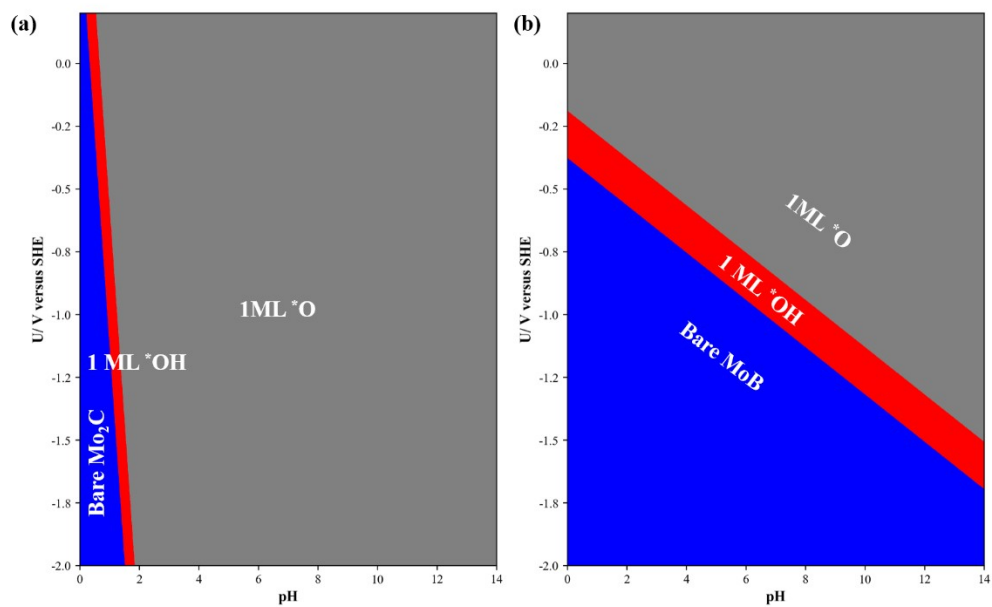


**Figure S2.** The calculated surface Pourbaix diagrams for (a)  $\text{Mo}_2\text{C}$  and (b)  $\text{MoB}$ .

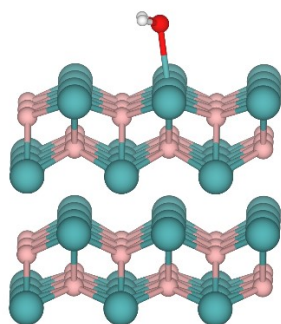


**Figure S3.** Optimized configuration of H<sub>2</sub>O adsorbed on MoB.

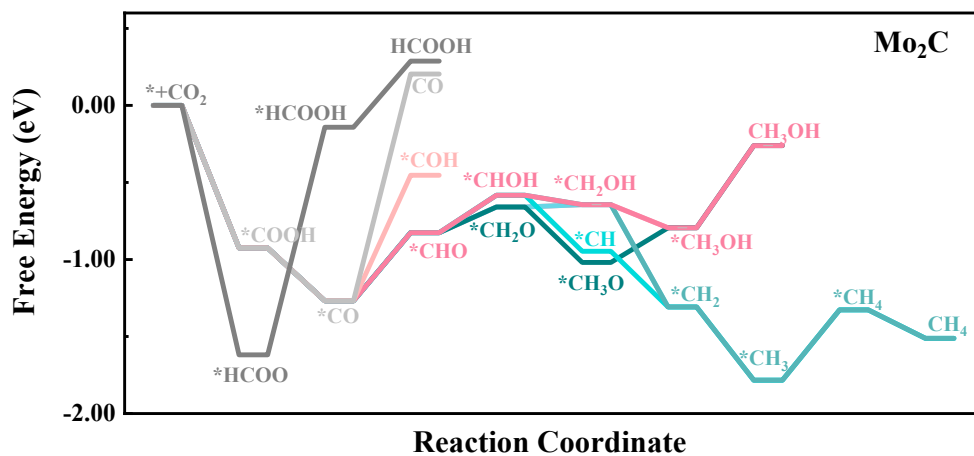


**Figure S4.** The CO<sub>2</sub>RR pathways to CO, HCOOH, CH<sub>3</sub>OH, and CH<sub>4</sub> on Mo<sub>2</sub>C at 0 V versus RHE.

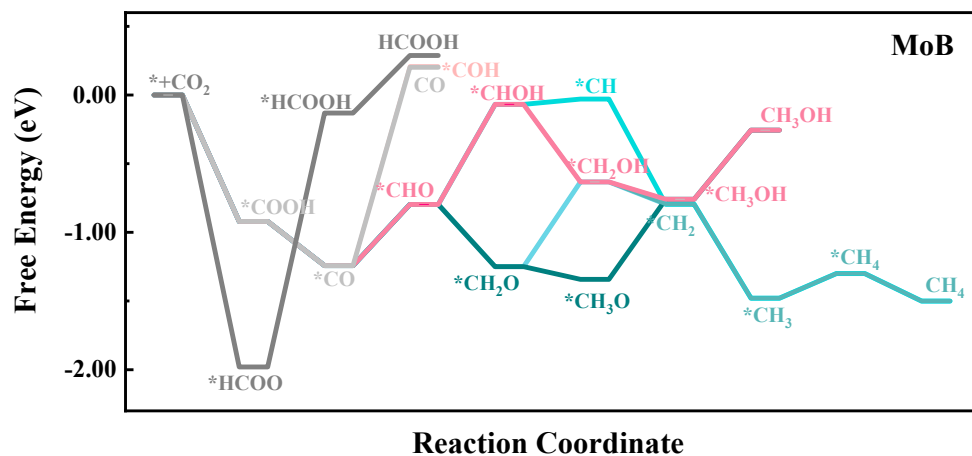


**Figure S5.** The CO<sub>2</sub>RR pathways to CO, HCOOH, CH<sub>3</sub>OH, and CH<sub>4</sub> on MoB at 0 V versus RHE.



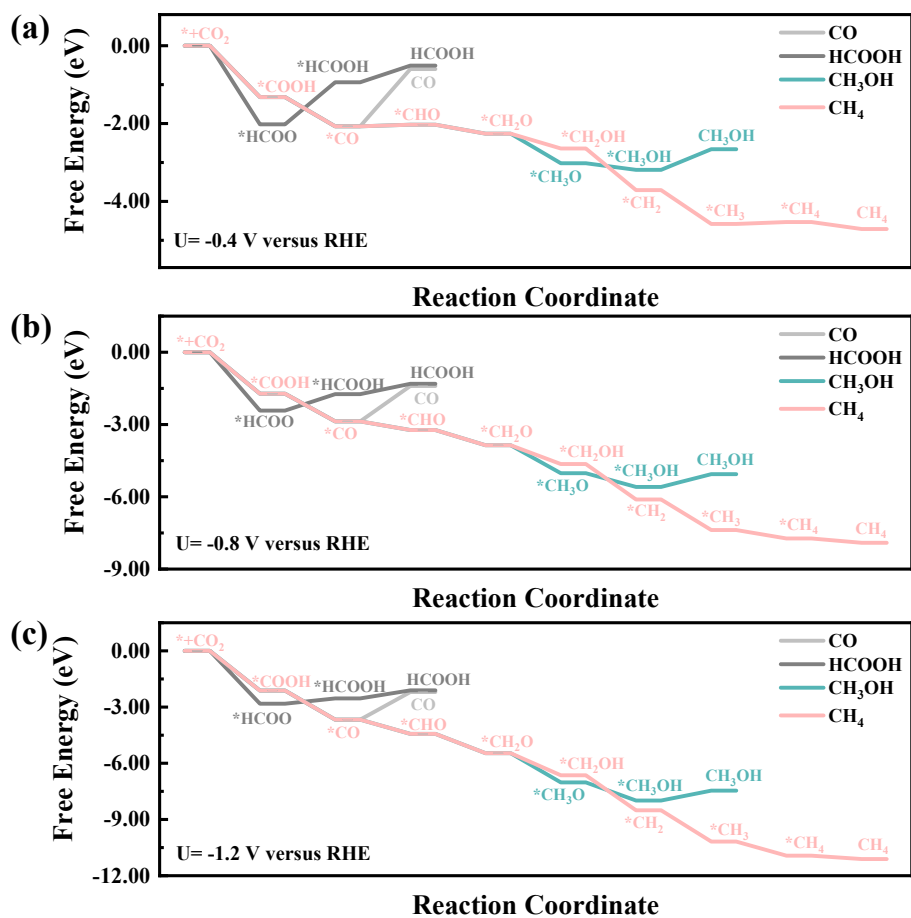


**Figure S6.** Free energy diagrams of CO<sub>2</sub>RR to CO, HCOOH, CH<sub>3</sub>OH, and CH<sub>4</sub> on Mo<sub>2</sub>C at different applied potentials, (a)  $U = -0.4$  V, (b)  $U = -0.8$  V, and (c)  $U = -1.2$  V versus RHE.

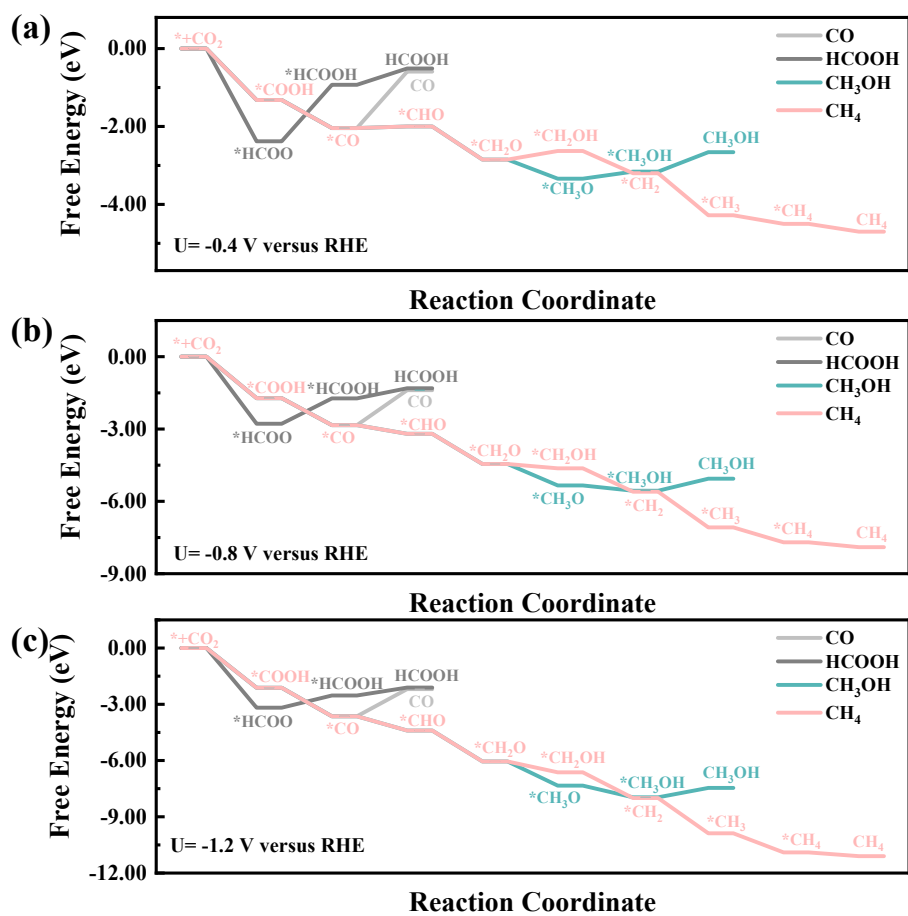


**Figure S7.** Free energy diagrams of CO<sub>2</sub>RR to CO, HCOOH, CH<sub>3</sub>OH, and CH<sub>4</sub> on MoB at different applied potentials, (a) U = -0.4 V, (b) U = -0.8 V, and (c) U = -1.2 V versus RHE.

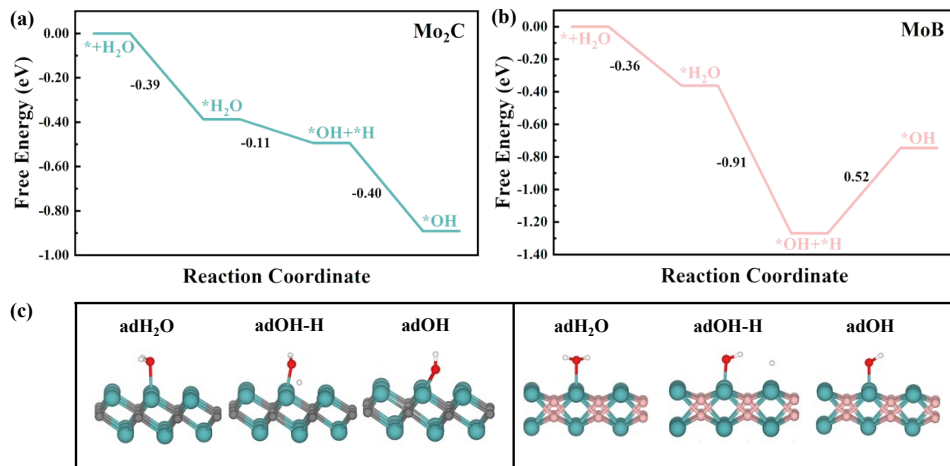


**Figure S8.** Hydrogen evolution reaction mechanisms in the alkaline electrolyte on (a) Mo<sub>2</sub>C and (b) MoB and (c) corresponding structural configurations.

**Table S1.** The Calculated (eV) and the experimental (eV) values of reaction potential at pH = 6.8 vs. RHE for CO<sub>2</sub>RR.

Half reaction	Calculated	Experimental
$\text{CO}_{2(\text{g})} + 2(\text{H}^+_{(\text{aq})} + \text{e}^-) \rightarrow \text{CO}_{(\text{g})} + \text{H}_2\text{O}_{(\text{l})}$	-0.12	-0.12
$\text{CO}_{2(\text{g})} + 2(\text{H}^+_{(\text{aq})} + \text{e}^-) \rightarrow \text{HCOOH}_{(\text{l})}$	-0.20	-0.20
$\text{CO}_{2(\text{g})} + 4(\text{H}^+_{(\text{aq})} + \text{e}^-) \rightarrow \text{HCHO}_{(\text{aq})} + \text{H}_2\text{O}_{(\text{l})}$	-0.07	-0.07
$\text{CO}_{2(\text{g})} + 6(\text{H}^+_{(\text{aq})} + \text{e}^-) \rightarrow \text{CH}_3\text{OH}_{(\text{aq})} + \text{H}_2\text{O}_{(\text{l})}$	0.03	0.03
$\text{CO}_{2(\text{g})} + 8(\text{H}^+_{(\text{aq})} + \text{e}^-) \rightarrow \text{CH}_{4(\text{g})} + 2\text{H}_2\text{O}_{(\text{l})}$	0.17	0.17

**Table S2.** Formation energy of Mo<sub>2</sub>C, Mo<sub>2</sub>CO<sub>2</sub>, and MoB.

Catalyst	Mo <sub>2</sub> C	Mo <sub>2</sub> CO <sub>2</sub>	MoB	MoBO <sub>2</sub>
Formation energy (eV/atom)	0.34	-1.13	-0.11	0.78

**Table S3.** Proposed elementary steps and free energy changes for CO<sub>2</sub>RR pathways on Mo<sub>2</sub>C and MoB at 0 V versus RHE.

Elementary steps	$\Delta G/\text{eV}$	
	Mo <sub>2</sub> C	MoB
$\text{H}^+ + \text{e}^- \rightarrow * \text{H}$	-0.21	-0.50
$\text{CO}_2 + \text{H}^+ + \text{e}^- \rightarrow * \text{COOH}$	-0.92	-0.92
$\text{CO}_2 + \text{H}^+ + \text{e}^- \rightarrow * \text{HCOO}$	-1.44	-1.98
$* \text{HCOO} + \text{H}^+ + \text{e}^- \rightarrow * \text{HCOOH}$	1.30	1.85
$* \text{HCOOH} \rightarrow * + \text{HCOOH}$	0.43	0.42
$* \text{COOH} + \text{H}^+ + \text{e}^- \rightarrow * \text{CO} + \text{H}_2\text{O}$	-0.34	-0.32
$* \text{CO} \rightarrow * + \text{CO}$	1.47	1.45
$* \text{CO} + \text{H}^+ + \text{e}^- \rightarrow * \text{COH}$	0.82	1.44
$* \text{CO} + \text{H}^+ + \text{e}^- \rightarrow * \text{CHO}$	0.44	0.45
$* \text{CHO} + \text{H}^+ + \text{e}^- \rightarrow * \text{CHOH}$	0.24	0.73
$* \text{CHO} + \text{H}^+ + \text{e}^- \rightarrow * \text{CH}_2\text{O}$	0.17	-0.45
$* \text{CHOH} + \text{H}^+ + \text{e}^- \rightarrow * \text{CH}_2\text{OH}$	-0.06	-0.57
$* \text{CHOH} + \text{H}^+ + \text{e}^- \rightarrow * \text{CH} + \text{H}_2\text{O}$	-0.36	0.04
$* \text{CH}_2\text{O} + \text{H}^+ + \text{e}^- \rightarrow * \text{CH}_3\text{O}$	-0.36	-0.09
$* \text{CH}_2\text{O} + \text{H}^+ + \text{e}^- \rightarrow * \text{CH}_2\text{OH}$	0.02	0.62
$* \text{CH}_3\text{O} + \text{H}^+ + \text{e}^- \rightarrow * \text{O} + \text{CH}_4$	-1.48	-1.07
$* \text{O} + \text{CH}_4 + \text{H}^+ + \text{e}^- \rightarrow * \text{OH} + \text{CH}_4$	0.10	0.18
$* \text{OH} + \text{CH}_4 + \text{H}^+ + \text{e}^- \rightarrow * \text{H}_2\text{O} + \text{CH}_4$	0.49	0.39
$* \text{H}_2\text{O} \rightarrow * + \text{H}_2\text{O}$	0.40	0.362
$* \text{CH}_2\text{OH} + \text{H}^+ + \text{e}^- \rightarrow * \text{CH}_2 + \text{H}_2\text{O}$	-0.66	-0.16
$* \text{CH}_2\text{OH} + \text{H}^+ + \text{e}^- \rightarrow * \text{CH}_3\text{OH}$	-0.15	-0.13
$* \text{CH}_3\text{OH} \rightarrow * + \text{CH}_3\text{OH}$	0.49	0.50
$* \text{CH} + \text{H}^+ + \text{e}^- \rightarrow * \text{CH}_2$	-0.36	-0.77
$* \text{CH}_2 + \text{H}^+ + \text{e}^- \rightarrow * \text{CH}_3$	-0.47	-0.68
$* \text{CH}_3 + \text{H}^+ + \text{e}^- \rightarrow * \text{CH}_4$	0.46	0.18
$* \text{CH}_4 \rightarrow * + \text{CH}_4$	-0.18	-0.20

**Table S4.** CO<sub>2</sub>RR products selectivity relevant to HER, all the CO<sub>2</sub>RR products selectivity are calculated by taking HER activity as a reference.

	Mo <sub>2</sub> C				MoB			
	0 V	-0.4 V	-0.8 V	-1.2 V	0 V	-0.4 V	-0.8 V	-1.2 V
CO	0	0	0.01%	23.76%	0	0	6.16%	99.37%
HCOOH	0	0.01%	99.84%	100%	0	0	99.37%	100%
CH <sub>3</sub> OH	0.43%	82.58%	99.99%	100%	17.42%	99.81%	100%	100%
CH <sub>4</sub>	0.77%	99.99%	100%	100%	8.83%	99.99%	100%	100%

## Reference

- [1] K.S. Exner, Design criteria for the competing chlorine and oxygen evolution reactions: avoid the OCl adsorbate to enhance chlorine selectivity, *Phys. Chem. Chem. Phys.*, 2020, **2**, 22451-22458.